

Marquette University

e-Publications@Marquette

Chemistry Faculty Research and Publications

Chemistry, Department of

9-2019

Evaluation of α -hydroxycinnamic Acids as Pyruvate Carboxylase Inhibitors

Daniel J. Burkett
Marquette University

Brittney N. Wyatt
Marquette University

Mallory Mews
Marquette University

Anson Bautista
Marquette University

Ryan Engel
Marquette University

See next page for additional authors

Follow this and additional works at: https://epublications.marquette.edu/chem_fac

 Part of the [Chemistry Commons](#)

Recommended Citation

Burkett, Daniel J.; Wyatt, Brittney N.; Mews, Mallory; Bautista, Anson; Engel, Ryan; Dockendorff, Chris; Donaldson, William A.; and St. Maurice, Martin, "Evaluation of α -hydroxycinnamic Acids as Pyruvate Carboxylase Inhibitors" (2019). *Chemistry Faculty Research and Publications*. 1001.
https://epublications.marquette.edu/chem_fac/1001

Authors

Daniel J. Burkett, Brittney N. Wyatt, Mallory Mews, Anson Bautista, Ryan Engel, Chris Dockendorff, William A. Donaldson, and Martin St. Maurice

Marquette University

e-Publications@Marquette

Chemistry Faculty Research and Publications/College of Arts and Science

This paper is NOT THE PUBLISHED VERSION; but the author's final, peer-reviewed manuscript. The published version may be accessed by following the link in the citation below.

Bioorganic & Medicinal Chemistry, Vol. 27, No. 18 (September 2019): 4041-4047. [DOI](#). This article is © Elsevier and permission has been granted for this version to appear in [e-Publications@Marquette](#). Elsevier does not grant permission for this article to be further copied/distributed or hosted elsewhere without the express permission from Elsevier.

Evaluation of α -hydroxycinnamic Acids as Pyruvate Carboxylase Inhibitors

Daniel J. Burkett

Department of Chemistry, Marquette University, Milwaukee, WI

Brittney N. Wyatt

Department of Biological Sciences, Marquette University, Milwaukee, WI

Mallory Mews

Department of Biological Sciences, Marquette University, Milwaukee, WI

Anson Bautista

Department of Chemistry, Marquette University, Milwaukee, WI

Ryan Engel

Department of Chemistry, Marquette University, Milwaukee, WI

Chris Dockendorff

Department of Chemistry, Marquette University, Milwaukee, WI

William A. Donaldson

Department of Chemistry, Marquette University, Milwaukee, WI

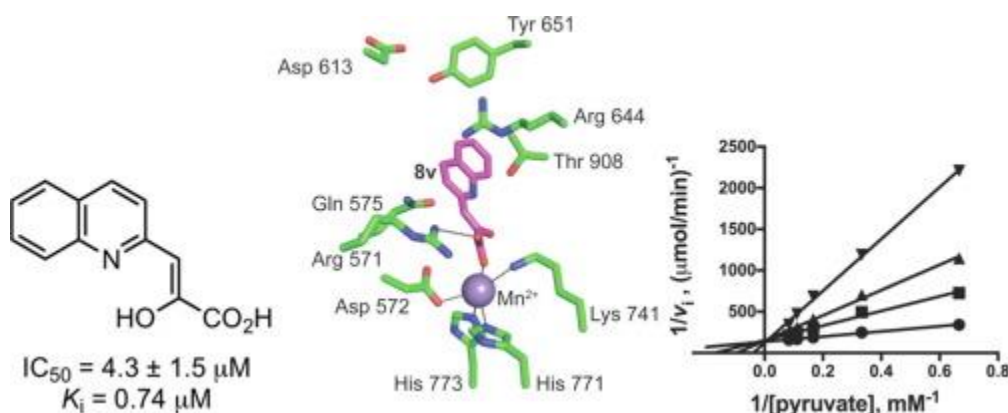
Martin St. Maurice

Department of Biological Sciences, Marquette University, Milwaukee, WI

Abstract

Through a structure-based drug design project (SBDD), potent small molecule inhibitors of pyruvate carboxylase (PC) have been discovered. A series of α -keto acids (**7**) and α -hydroxycinnamic acids (**8**) were prepared and evaluated for inhibition of PC in two assays. The two most potent inhibitors were 3,3'-(1,4-phenylene)bis[2-hydroxy-2-propenoic acid] (**8u**) and 2-hydroxy-3-(quinoline-2-yl)propenoic acid (**8v**) with IC_{50} values of $3.0 \pm 1.0 \mu\text{M}$ and $4.3 \pm 1.5 \mu\text{M}$ respectively. Compound **8v** is a competitive inhibitor with respect to pyruvate ($K_i = 0.74 \mu\text{M}$) and a mixed-type inhibitor with respect to ATP, indicating that it targets the unique carboxyltransferase (CT) domain of PC. Furthermore, compound **8v** does not significantly inhibit human carbonic anhydrase II, matrix metalloproteinase-2, malate dehydrogenase or lactate dehydrogenase.

Graphical abstract



Keywords

Pyruvate carboxylase, Carboxyltransferase, α -Hydroxycinnamic acids, α -Keto acids

1. Introduction

Pyruvate carboxylase (PC) is an important anaplerotic enzyme that catalyzes the conversion of pyruvate to oxaloacetate (OAA) in a wide range of organisms.¹ Studies have linked PC activity to a number of diseases and infections including certain types of cancer,^{2a} type 2 diabetes,^{2b} and listeriosis^{2c} that are sustained as a result of aberrant or essential PC expression in cells. Genetic manipulations of PC have validated it as a potential target for the treatment of these diseases and infections, but genetic tools alone are insufficient to identify the precise mechanistic role that PC plays *in vivo*. Specific and potent small molecule effectors of PC can alter the catalytic activity without reducing or eliminating the gene product from the cellular system, thus precluding unintentional effects on associated metabolic and signaling enzymes in the cell. To date, attempts to use small molecule effectors to study PC directly in cellular studies have made use of unselective inhibitors of PC

expression/activity, all of which have the potential to interact with multiple cellular systems.³ For example phenylacetate has been applied as a PC inhibitor in studies of insulin release.⁴ However, the high concentrations (>5 mM) required to partially inhibit PC are expected to impact many other cellular processes, including the induction of cell cycle arrest,^{5a,b} and inhibition of nitric oxide synthase.^{5c}

The MgATP-dependent carboxylation of pyruvate by HCO_3^- to form OAA occurs in two distinct active sites of PC: the biotin carboxylation (BC) domain that is conserved across all biotin dependent carboxylases,⁶ and the unique carboxyltransferase (CT) domain that, outside of PC, is found in only a few bacterial oxaloacetate decarboxylases.⁷ The biotin cofactor, which is covalently attached to the biotin carboxyl carrier protein (BCCP) domain, is carboxylated in the BC domain, and subsequently transferred to the CT domain where pyruvate is carboxylated to form OAA. A structure-based project was initiated to develop chemical probes that will target the CT domain of PC. We describe here the discovery of promising first generation small molecule PC inhibitors and their kinetic characterization.

2. Results and discussion

Both substrates and inhibitors of the CT domain of PC can promote carboxybiotin decarboxylation.⁸ Binding of CT domain ligands facilitates a structural rearrangement which allows carboxybiotin to access the CT domain active site and decarboxylate.⁹ Fluoropyruvate (**1a**, Fig. 1), hydroxypyruvate (**1b**), oxamate (**2**) and glyoxylate (**3**) all promote carboxybiotin decarboxylation,⁸ and crystal structures of PC with pyruvate, 3-bromopyruvate (**1c**), oxalate (**4**), **1b**, and **2** reveal that these molecules bind with overlapping orientations of their α -keto acid functional groups in the CT domain active site.¹⁰

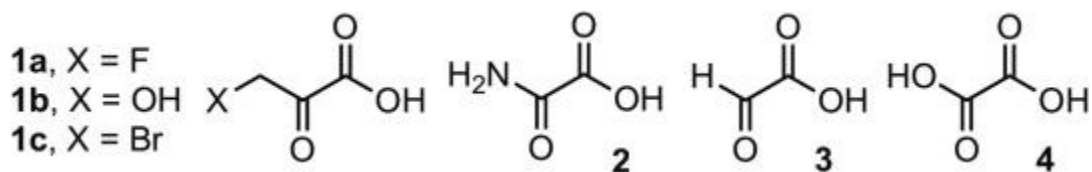


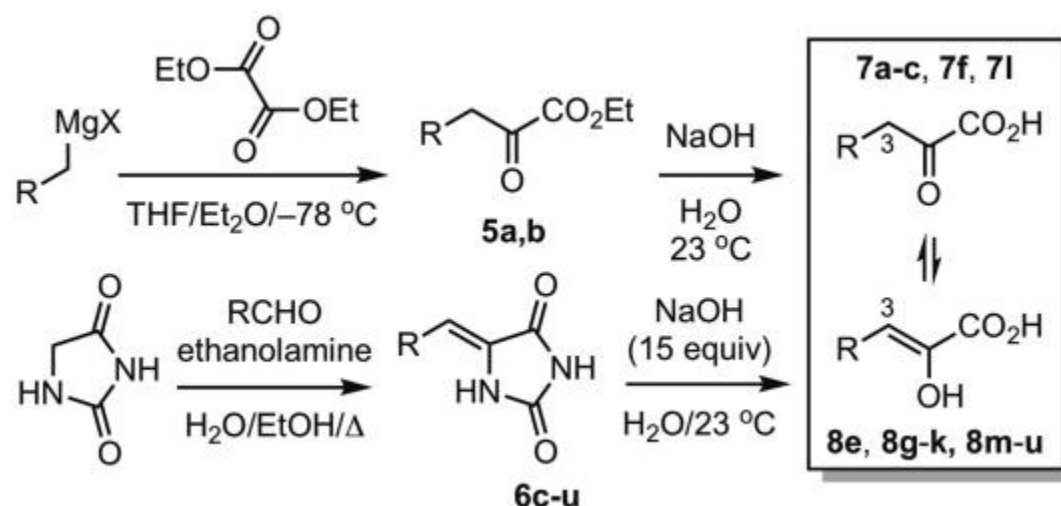
Fig. 1. Known inhibitors of pyruvate carboxylase.

In parallel with efforts to screen compound libraries,¹¹ we endeavored to identify inhibitors by taking the classical approach of modifying the enzymatic substrate. We reasoned that the range of known α -keto acid PC inhibitors and their related X-ray structures would also support a structure-based approach that could help to identify larger α -keto acids inhibitors of PC, but with higher potency and selectivity. Our overall objective is to identify probes with suitable potency, selectivity and physico/physiochemical properties for *in vivo* studies.

2.1. Compound synthesis

Two routes were employed for the preparation of α -keto acids/substituted α -hydroxycinnamic acids (Scheme 1). Addition of one equivalent of a Grignard reagent to diethyl oxalate in ether/THF at -78°C , followed by aqueous quench at low temperature afforded the corresponding α -ketoesters **5a-b**.¹² Alternatively, heating a mixture of hydantoin and cyclohexane-carboxaldehyde or substituted benzaldehydes in ethanol/water afforded the corresponding 5-methylene-2,4-imidazolidinediones **6c-u**, which generally precipitated during the Knoevenagel condensation.¹³ Base hydrolysis of α -

ketoesters **5a-b** or of 5-methylene-2,4-imidazolidinediones **6c-u** gave the corresponding α -keto acids (**7**) or substituted α -hydroxycinnamic acids (**8**).

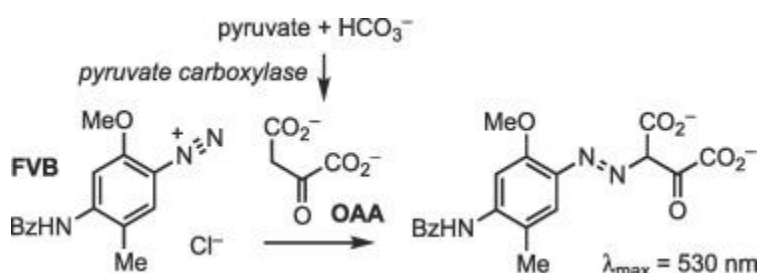


Scheme 1. Syntheses of α -ketoacids/ α -hydroxycinnamic acids.

The parent, *m*- and *p*-substituted 3-arylpyruvic acids **8e**, **8g-k**, and **8m-v** were found to exist predominantly in the enol form (i.e. α -hydroxycinnamic acid), while the alkyl substituted pyruvic acids **7a-c** and the *o*-substituted 3-arylpyruvic acids **7f** and **7l** exist predominantly in the keto form. These assignments are based on NMR spectral data. In particular, signals at ca. δ 107 and at ca. δ 6.4 ppm (s, 1H) in the ^{13}C and ^1H NMR spectra of compounds **8** (in d_6 -DMSO) correspond to C3 and its attached proton of the enol structures, while signals at ca. δ 30 and at ca. δ 3 ppm in the ^{13}C and ^1H NMR spectra of compounds **7** (in d_6 -DMSO) correspond to C3 and its attached proton of the keto structures. Similar keto-enol distribution has been previously observed in CD_3CN .¹⁴

2.2. PC inhibition assays

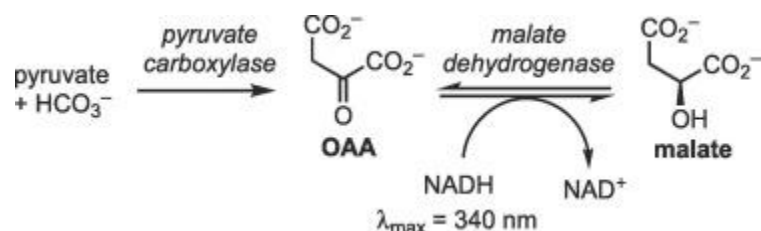
While human PC represents the ideal target for these studies, it has proven to be extremely difficult to obtain workable yields of full-length, recombinant human PC.^{9a} Instead, compounds were initially screened for inhibition of *Staphylococcus aureus* PC (*Sa*PC) using an optimized fixed-time assay¹¹ that is based on the reaction of OAA, the product of the PC-catalyzed reaction, with Fast Violet B (FVB), a diazonium salt which produces a colored adduct with an absorbance maximum at 530 nm (Scheme 2).



Scheme 2. Detection of OAA production by reaction with FVB.

As a secondary assay to confirm *Sa*PC inhibition, the carboxylation of pyruvate in full-length *Sa*PC was measured by coupling the formation of OAA to the reaction catalyzed by malate dehydrogenase

(MDH), which converts OAA to malate and oxidizes NADH to NAD⁺ (Scheme 3). This can be readily observed by measuring the change in absorbance of NADH at 340 nm.



Scheme 3. Detection of OAA production by a malate dehydrogenase (MDH) coupled enzyme assay.

Compounds which existed predominantly as the α -keto acids (**7a-d**, Fig. 2; **7f** and **7l**, Table 1) as well as 3-phenyllactic acid (**9**) had negligible inhibitory activity ($\text{IC}_{50} > 1000 \mu\text{M}$). In contrast, those compounds which existed as enols (α -hydroxycinnamic acids), such as phenylpyruvic acid (**8e**, $\text{IC}_{50} = 240 \mu\text{M}$, Table 1), exhibited promising inhibitory activity in the FVB assay. The higher inhibition of enols over α -keto acids is consistent with the predicted pyruvate enolate intermediate in the CT domain reaction mechanism, suggesting that the high affinity of these compounds comes from their ability to serve as intermediate analogs. As such, these results are consistent with the CT domain as the target of these compounds. While α -hydroxycinnamic acid **8g** bearing a strongly electron withdrawing *para*-nitro group exhibited only weak inhibitory activity, the corresponding α -hydroxycinnamic acid bearing a *para*-CF₃ group (**8k**) inhibited pyruvate with $\text{IC}_{50} = 130 \mu\text{M}$ in the FVB assay. There does not appear to be a strong correlation between the electron withdrawing/electron donating ability of *para*-substituents and inhibitory activity. The two most potent inhibitors were 3,3'-(1,4-phenylene)bis[2-hydroxy-2-propenoic acid] (**8u**) and 2-hydroxy-3-(quinoline-2-yl)propenoic acid (**8v**) with IC_{50} values of $3.0 \pm 1.0 \mu\text{M}$ and $4.3 \pm 1.5 \mu\text{M}$ respectively. IC_{50} values determined in the MDH coupled assay were generally slightly lower than those determined in the FVB assay, but the values from these two assays correlated well.

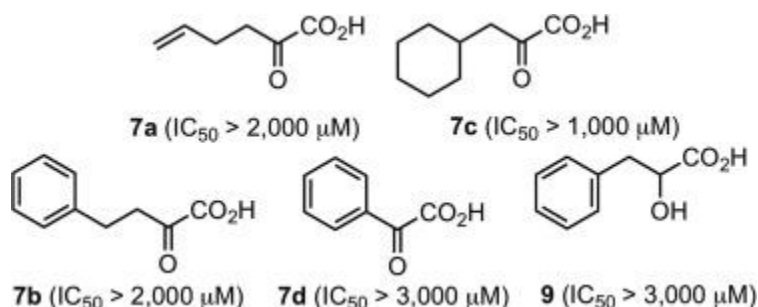
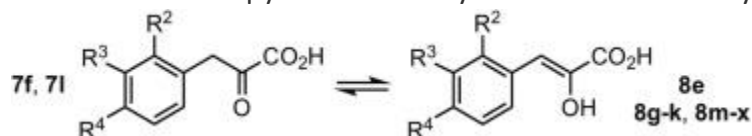
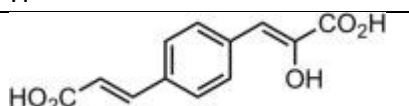
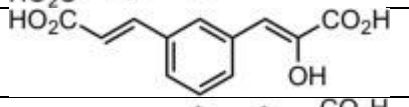
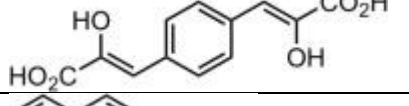
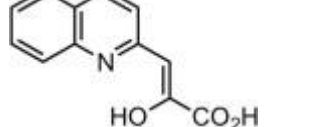


Fig. 2. Compounds which exist predominantly in the α -keto acid form (**7a-7d**) and 3-phenyllactic acid (**9**) exhibit weak inhibitor activity against *Sa*PC (FVB assay).

Table 1. *S. aureus* pyruvate carboxylase inhibition activity (IC_{50} values in μM).



	R ²	R ³	R ⁴	FVB IC ₅₀	MDH IC ₅₀
8e	H	H	H	240	130
7f	NO ₂	H	H	>2000	>2000
8g	H	H	NO ₂	>1000	>1000
8h	H	Me	H	360	23
8i	H	H	Me	210	140
8j	H	Me	Me	98	38
8k	H	H	CF ₃	130	96
7l	Br	H	H	>1000	>1000
8m	H	H	Br	200	81
8n	H	H	Cl	280	220
8o	H	H	F	100	30
8p	H	H	OMe	170	56
8q	H	H	OH	67	22
8r	H	H	3-thienyl	48.0	–
8s				58.6	–
8t				118	–
8u				3.0 ± 1.0	11
8v				4.3 ± 1.5	3.2 ± 0.5

2.3. Determination of mode of inhibition

Steady-state kinetic analysis was used to determine the K_i value and mode of inhibition for one of the most potent compounds (**8v**). It was determined to be a competitive inhibitor with respect to pyruvate with a $K_i = 0.74 \mu\text{M}$, and a mixed-type inhibitor with respect to ATP with $K_i = 5.2 \mu\text{M}$ (Fig. 3). As an additional measure to assess whether our procedure for determining K_i values was accurate, predictive K_i values were determined with the Cheng-Prusoff equation for competitive inhibition for **8v** ($0.46 \mu\text{M}$) and oxalate ($0.43 \mu\text{M}$). The close match of the predictive and kinetically determined K_i values, as well as the unaltered binding affinity with increased concentration of ATP is consistent with direct competition of **8v** with pyruvate in the CT domain active site. Identical modes of inhibition were observed against ATP and pyruvate for oxalate and for **8i**, suggesting that α -hydroxycinnamic acids specifically target the CT domain for inhibition (Supplementary Fig. S1).

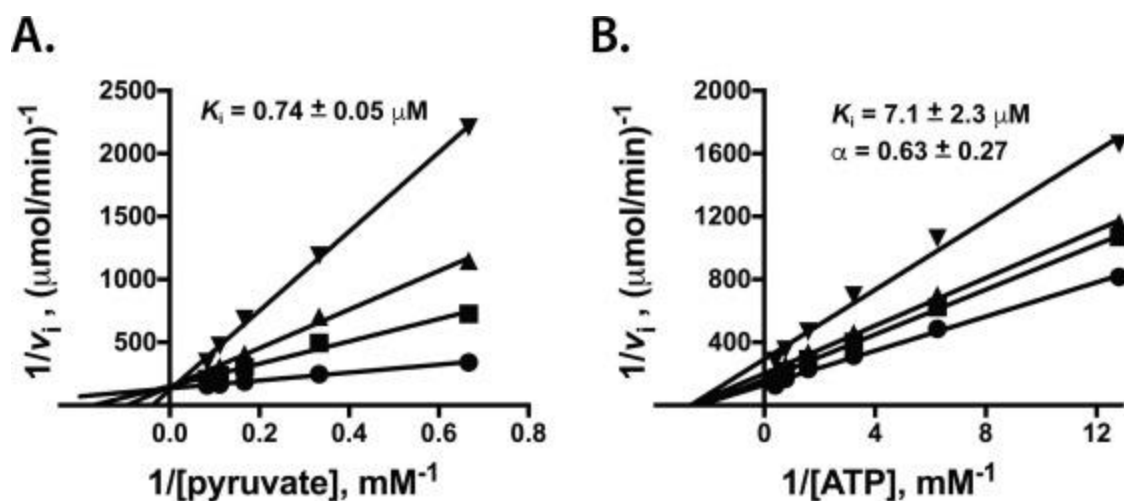


Fig. 3. Compound **8v** is a competitive inhibitor with respect to pyruvate and a mixed-type inhibitor with respect to ATP. A) A double-reciprocal plot demonstrating competitive inhibition of **8v** with respect to pyruvate, K_i value = $0.74 \mu\text{M}$. B) A double-reciprocal plot demonstrating mixed-type inhibition of **8v** with respect to ATP, K_i value = $5.2 \mu\text{M}$. Initial velocities were determined at the following concentrations of **8v**: 0 μM (circles), 1.5 μM (squares), 3 μM (upright triangles) and 6 μM (inverse triangles). The reported K_i values, α values and standard errors are determined from global fits of the data to the equations for reversible competitive or mixed-type inhibition.

2.4. Docking studies

Computational docking was conducted using the CT domain structure from *S. aureus* PC (pdb code 3BG5) to predict the relative binding affinity and poses of the most potent inhibitors for the CT domain of PC, and to visualize the predicted binding site. Upon the binding of pyruvate, the CT domain adopts a closed conformation where the carboxy moiety of pyruvate forms a salt bridge with the guanidinium side-chain of Arg644 (human PC numberings are used throughout) and the carbonyl oxygen of pyruvate is within hydrogen bonding distance of Arg571 and Gln575. These residues contribute to stabilizing the enolpyruvate intermediate. In the closed conformation, Tyr651 hydrogen bonds with Asp613.¹⁵ Due to the predicted importance of the enol moiety of the α -hydroxy-3-arylcinnamic acids, all compounds were docked in their enol form. In the docking pose of **8u** and **8v**, with PC in the closed conformation, the carboxyl moieties are not positioned such that they form salt bridges with Arg644, but rather both are oriented such that the carboxyl groups are coordinated with the metal ion in the center of the CT domain active site (Fig. 4A and C). This interaction with Mn^{2+} contributes to an octahedral coordination, which is consistent with what has been observed in multiple crystal structures of PC. The carboxy moiety coordinated to the metal ion of both **8u** and **8v** is within hydrogen bonding distance of Arg571. Notably, docking studies predict both the α -enolic carboxyl moiety of **8u** that is not predicted to coordinate the metal ion and the fused quinolinyl ring of **8v** occupy the space that biotin has been shown to occupy in several X-ray crystal structures (see Fig. 4B and D).⁹

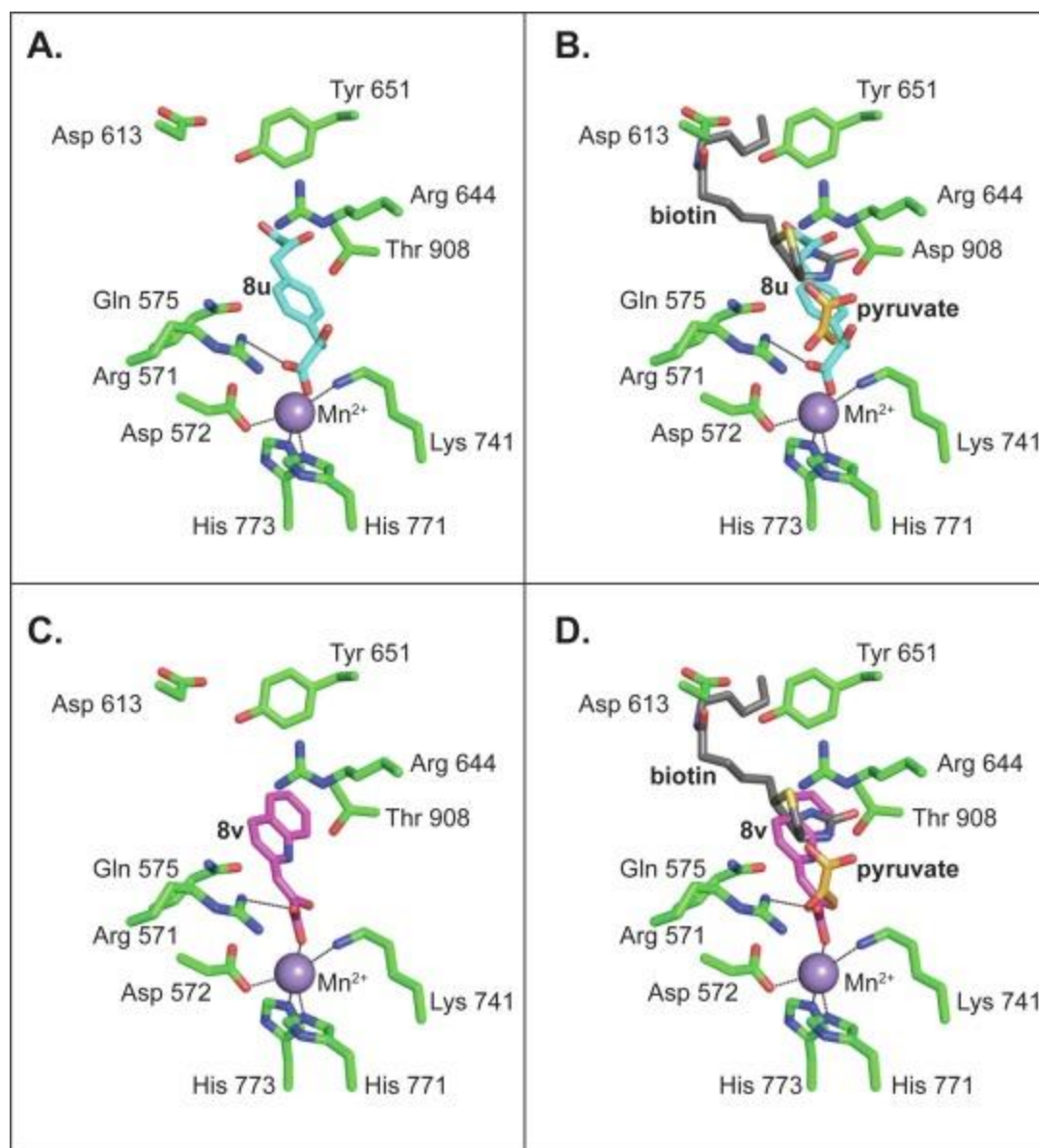


Fig. 4. A) Docking pose of **8u** in the closed conformation of the CT domain without biotin present. The Mn^{2+} metal ion is represented by the grey sphere. B) Overlay of docked structure with the crystal structure showing the α -enolic carboxyl moiety of **8u** that is not predicted to coordinate the metal ion occupies the binding location of biotin. C) Docking pose of **8v** in the closed conformation of the CT domain without biotin present. D) Overlay of docked structure with the crystal structure showing the quinolinyl ring **8v** occupies the binding location of biotin. Residues are numbered according to the sequence of human PC.

2.5. Evaluation of **8u** and **8v** against hCAII, MMP-2, MDH and LDH

The docking studies predicted that the α -keto acid moiety directly coordinates with the metal ion, raising questions about the selectivity of this class of compounds for PC inhibition. Selectivity was evaluated using two common metalloenzymes, human carbonic anhydrase 2 (*hCAII*) and matrix metalloproteinase 2 (MMP-2). While the potent PC inhibitor **8v** did not appreciably inhibit *hCAII* at 200 μ M or MMP-2 activity at 50 μ M (Fig. 5), compounds **8u** and **8s** increased the activity of *hCAII*,

while **8u**, **8s**, and **8r** exhibited substantial inhibition of MMP-2 at 50 μM . It is reassuring that **8v** also did not inhibit enzymes that act on similar substrates: MDH (Supplementary Table S1, Supplementary Fig. S2) and lactate dehydrogenase (LDH) (Supplementary Fig. S2, Supplementary Fig. S3), nor is it used as a substrate of LDH (Supplementary Fig. S4).

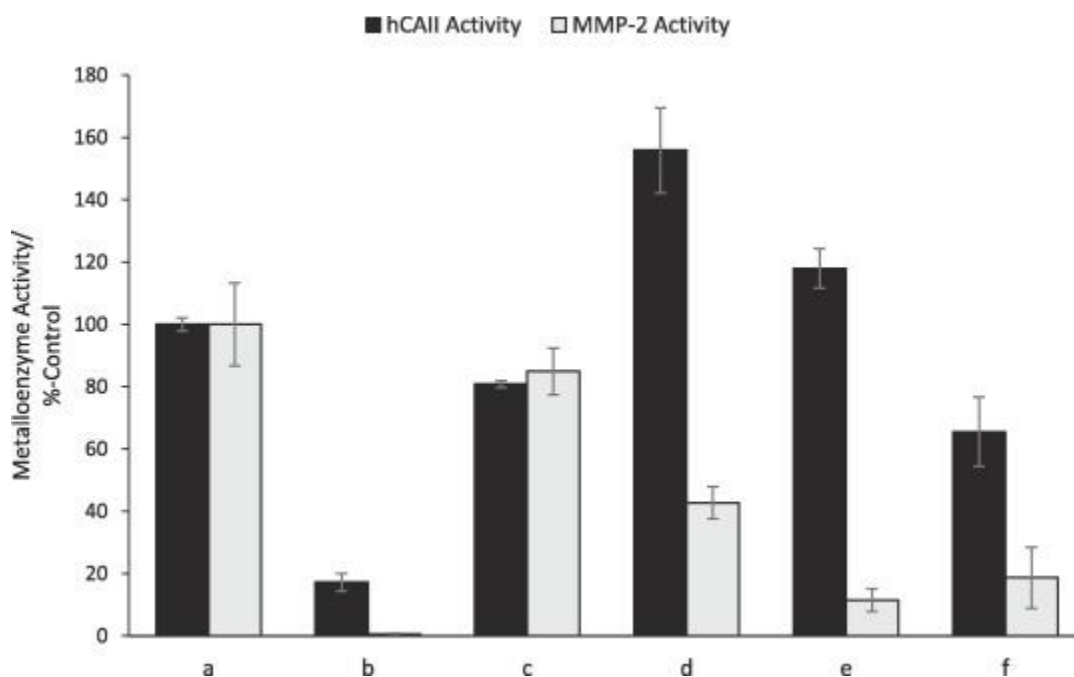


Fig. 5. Activity of human carbonic anhydrase II (*hCAII* = black bars) in the presence of compounds (200 μM) or matrix metalloproteinase-2 (MMP-2 = grey bars) in the presence of compounds (50 μM). (a) Negative control, (b) known inhibitor (acetazolamide, 5 μM for *hCAII*; PD166793, 100 μM for MMP-2), (c) **8v**, (d) **8u**, (e) **8s**, (f) **8r**. Error bars represent standard error of the mean for four determinations each.

3. Conclusions

Building off the common binding motif observed for α -keto acids in the CT domain active site of PC, we synthesized and evaluated a series of α -hydroxycinnamic acids as a new class of PC inhibitors.

Compared to previously characterized inhibitors of PC, these demonstrate improved potency and, for **8v**, promising initial selectivity that serves as a good starting point for the continued development of small molecule probes directed against PC. Such probes will be enormously useful in evaluating the metabolic role of PC in the onset and progression of diseases such as type 2 diabetes and cancer.

Future structure-based efforts will seek to further improve the design of molecular properties en route to producing the first class of potent and selective inhibitors of this important metabolic enzyme.

4. Experimental

4.1. Chemistry

4.1.1. General experimental

All reactions involving moisture or air sensitive reagents were carried out under a nitrogen atmosphere in oven-dried glassware with anhydrous solvents. THF and ether were distilled from

sodium/benzophenone. Purifications by chromatography were carried out using flash silica gel (32–63 μ). NMR spectra were recorded on either a Varian Mercury+ 300 MHz or a Varian UnityInova 400 MHz instrument. CDCl_3 and d_6 -DMSO was purchased from Cambridge Isotope Laboratories. ^1H NMR spectra were calibrated to 7.27 ppm for residual CHCl_3 or 2.50 ppm for d_5 -DMSO. ^{13}C NMR spectra were calibrated from the central peak at 77.23 ppm for CDCl_3 or 39.52 ppm for d_6 -DMSO. Coupling constants are reported in Hz. Elemental analyses were obtained from Midwest Microlabs, Ltd., Indianapolis, IN, and high-resolution mass spectra were obtained from the COSMIC lab at Old Dominion University.

Ethyl 2-oxo-5-hexenoate (**5a**)^{12a} and ethyl 2-oxo-4-phenylbutanoate (**5b**)^{12b} were prepared by literature procedures. Methyl 4'-formylcinnamate and methyl 3'-formylcinnamate were prepared by Pd-catalyzed Heck coupling of methyl acrylate with either 4-bromobenzaldehyde or 3-bromobenzaldehyde, and were identified by comparison to literature spectral data.¹⁶ 4-(3-Thienyl)benzaldehyde was prepared by Pd-catalyzed Suzuki coupling of 3-thiophene boronic acid with 4-bromobenzaldehyde, and was identified by comparison to literature spectral data.¹⁶ Phenylglyoxylic acid (**7d**), (2-nitrophenyl)pyruvic acid (**7f**), 2-hydroxy-3-(4-hydroxyphenyl)-2-propenoic acid (**8q**) and 3-phenyllactic acid (**9**) were purchased from Sigma-Aldrich, and 2-hydroxy-3-(quinolin-2-yl)propenoic acid (**8v**) was purchased from Enamine Building Blocks.

4.1.2. General procedure for hydrolysis of α -ketoesters

To compounds **5a-b**, a solution of excess 2.5 N NaOH was added. The aqueous mixture was stirred at room temperature until the initially emulsified mixture reached uniformity, at least 12 h. The reaction mixture was quenched with 1 N HCl, and the resulting α -keto acids were extracted several times with ether, and the combined organic layers washed with brine, dried (MgSO_4) and concentrated to give the corresponding product

4.1.3. 2-Oxohex-5-enoic acid (**7a**)

The hydrolysis of **5a** (60 mg, 0.38 mmol) by the general procedure gave **7a** as a yellow oil (14 mg, 29%). ^1H NMR (400 MHz, CDCl_3) δ 5.80–5.65 (m, 1H), 5.04–4.91 (m, 2H), 2.98 (t, $J = 7.2$ Hz, 2H), 2.44–2.30 (m, 2H) ^{13}C NMR (100 MHz, CDCl_3) δ 195.1, 160.0, 135.8, 116.2, 36.7, 26.6 ppm.

4.1.4. 2-Oxo-4-phenylbutanoic acid (**7b**)

The hydrolysis of **5b** (52 mg, 0.25 mmol) by the general procedure gave **7b** as a yellow oil (29 mg, 56%). ^1H NMR (400 MHz, CDCl_3) δ 7.33–7.17 (m, 5H), 3.21 (t, $J = 7.6$ Hz, 2H), 2.96 (t, $J = 7.6$ Hz, 2H); ^{13}C NMR (100 MHz, CDCl_3) δ 195.4, 161.1, 140.1, 128.6, 128.4, 126.4, 40.1, 29.0 ppm. The spectral data for this compound was consistent with the literature values.¹⁷

4.1.5. General procedure for preparation of substituted 5-methylenehydantoin

Hydantoin (500 mg, 5 mmol) was dissolved in H_2O (50 mL) at 70 $^\circ\text{C}$ with stirring. Ethanolamine (0.61 mL) was added to the mixture, which was then heated to reflux. An equimolar quantity of the appropriate aldehyde solution (5 mmol in 5 mL ethanol) was added dropwise. The reaction mixture was heated at reflux for 5 h. The mixture was cooled to room temperature, during which time the product precipitated. The precipitate was collected via vacuum filtration, washed several times with H_2O and dried *in vacuo*. Compounds **6c**, **6e-i**, and **6k-p** were prepared by the procedure and their NMR spectral data was consistent with the literature values.^{13a}

4.1.6. 5-(3,4-Dimethylphenyl)methylene-2,4-imidazolidinedione (6j)

Condensation of 3,4-dimethylbenzaldehyde (671 mg, 5.00 mmol) by the general procedure gave **6j** (653 mg, 60%) as a white solid. mp > 215 °C; ¹H NMR (400 MHz, *d*₆-DMSO) δ 11.08–10.47 (br s, 2H), 7.38 (s, 1H), 7.27 (d, *J* = 7.9 Hz, 1H), 7.10 (d, *J* = 7.9 Hz, 1H), 6.30 (s, 1H), 2.19 (s, 3H), 2.17 (s, 3H); ¹³C NMR (100 MHz, *d*₆-DMSO) δ 166.2, 156.1, 137.5, 137.2, 130.8, 130.4, 130.3, 127.7, 127.4, 109.2, 19.7, 19.5 ppm. Anal. Calcd. For C₁₂H₁₂N₂O₂: C, 66.65; H, 5.59; N, 12.93. Found: C, 66.87; H, 5.54; N, 13.10.

4.1.7. 5-[4-(3-Thienyl)phenyl]methylene-2,4-imidazolidinedione (6r)

Condensation of 4-(3-thienyl)benzaldehyde (498 mg, 2.65 mmol) by the general procedure gave **6r** (560 mg, 78%) as a beige solid. mp > 215 °C; ¹H NMR (300 MHz, *d*₆-DMSO) δ 8.28 (s, 1H), 7.93 (s, 1H), 7.76 (d, *J* = 3.9 Hz, 1H), 7.74–7.70 (m, 2H), 7.64 (s, 1H), 7.62–7.57 (m, 2H), 6.34 (s, 1H); ¹³C NMR (75 MHz, *d*₆-DMSO) δ 162.0, 157.3, 141.7, 135.6, 132.5, 130.3, 129.1, 128.1, 126.5, 122.6, 122.3, 107.9.

4.1.8. 5-(4-(2-Methoxycarbonyl)ethenylphenyl)methylene-2,4-imidazolidinedione (6s)

Condensation of methyl 4'-formylcinnamate (554 mg, 2.91 mmol) by the general procedure gave **6s** (369 mg, 47%) as a pale yellow solid. mp > 215 °C; ¹H NMR (400 MHz, *d*₆-DMSO) δ 11.31 (s, 1H), 10.69 (s, 1H), 7.67 (d, *J* = 8.0 Hz, 2H), 7.61 (d, *J* = 8.0 Hz, 2H), 7.53 (d, *J* = 15.4 Hz, 1H), 6.55 (d, *J* = 15.4 Hz, 1H), 6.37 (s, 1H), 3.53 (s, 3H); ¹³C NMR (100 MHz, *d*₆-DMSO) δ 168.1, 165.9, 156.1, 143.6, 135.2, 134.4, 130.2, 129.0, 128.3, 120.1, 107.8, 57.8.

4.1.9. 5-(3-(2-Methoxycarbonyl)ethenylphenyl)methylene-2,4-imidazolidinedione (6t)

Condensation of methyl 3'-formylcinnamate (537 mg, 2.44 mmol) by the general procedure gave **6t** (409 mg, 53%) as a yellow solid. mp 232–235 °C; ¹H NMR (400 MHz, *d*₆-DMSO) δ 8.27–8.14 (m, 1H), 7.84 (s, 1H), 7.77 (s, 1H), 7.59 (d, *J* = 16.4 Hz, 1H), 7.57–7.47 (m, 1H), 7.41 (t, *J* = 6.8 Hz, 1H), 7.25 (t, *J* = 6.8 Hz), 6.65 (d, *J* = 16.4 Hz, 1H), 6.39 (s, 1H), 3.20 (s, 3H); ¹³C NMR (100 MHz, *d*₆-DMSO) δ 166.3, 165.8, 156.3, 139.0, 136.5, 134.0, 132.6, 129.8, 129.0, 127.2, 123.4, 121.7, 108.0, 60.3. HRMS (FAB): (M₂ + Na⁺) found 567.1487. (C₁₄H₁₂N₂O₄)₂Na requires 567.1486.

4.1.10. 5,5'-(1,4-Phenylenedimethylidene)bis[2,4-imidazolidinedione] (6u)

Condensation of 1,4-benzenedicarboxaldehyde (671 mg, 5.00 mmol) by the general procedure was modified by the use of two equivalents of hydantoin (1.011 g, 10.10 mmol) gave **6u** (442 mg, 30%) as a white solid. mp > 215 °C; ¹H NMR (300 MHz, *d*₆-DMSO) δ 10.89 (br s, 4H), 7.63 (s, 4H), 6.40 (s, 2H).

4.1.11. General procedure for hydrolysis of benzylhydantions

To a suspension of the benzylhydantoin in H₂O (25 mL) was added solid NaOH (15 equivalents). The mixture was heated at reflux for 12 h under an N₂ atmosphere, during which time the material went into solution. After cooling to room temperature, the stirred reaction mixture was quenched with concentrated HCl. The mixture was extracted several times with ether. The combined extracts were dried (MgSO₄) and concentrated to give the α-keto acid/2-hydroxy-3-arylcinnamic acid.

Compounds **7c**, **7l**¹⁴, **8e**^{13c}, **8g**^{13d}, **8h**^{13c}, **8i**^{13c}, **8k**^{13f}, **8n**^{13f}, **8o**^{13e}, **8p**^{13f}, were prepared by the procedure and their NMR spectral data was consistent with the literature values.

The following compounds were prepared by this procedure:

4.1.12. 3-(3,4-Dimethylphenyl)-2-hydroxy-2-propenoic acid (8j)

Hydrolysis of **6j** (424 mg, 1.99 mmol) by the general procedure gave **8j** (206 mg, 55%) as an orange solid. mp 134–136 °C; ¹H NMR (400 MHz, *d*₆-DMSO): δ 9.90 (s, 1H), 7.60 (d, *J* = 7.6 Hz, 2H), 7.33 (d, *J* = 7.6 Hz, 2H), 6.64 (s, 1H), 2.23 (s, 3H), 2.18 (s, 3H); ¹³C NMR (100 MHz, *d*₆-DMSO) δ 167.0, 141.4, 136.4, 136.0, 132.9, 130.8, 129.9, 127.4, 110.4, 19.9, 19.7 ppm. HRMS (FAB): M+Na⁺, found 215.0675. C₁₁H₁₂O₃Na requires 215.0678.

4.1.13. 3-(4-Bromophenyl)-2-hydroxy-2-propenoic acid (8m)

Hydrolysis of **6m** (403 mg, 1.51 mmol) by the general procedure gave **8m** (99 mg, 27%) as a white solid. mp 194–196 °C; ¹H NMR (400 MHz, *d*₆-DMSO): δ 9.49 (s, 1H), 7.69 (d, *J* = 8.6 Hz, 2H), 7.51 (d, *J* = 8.6 Hz, 2H), 6.36 (s, 1H); ¹³C NMR (100 MHz, *d*₆-DMSO) δ 166.5, 143.1, 134.7, 131.7, 131.6, 120.5, 108.5 ppm. HRMS (FAB): M+Na⁺, found 264.9470. C₉H₇O₃BrNa requires 264.9471.

4.1.14. 2-Hydroxy-3-[4-(3-thienyl)phenyl]-2-propenoic acid (8r)

Hydrolysis of **6r** (493 mg, 1.83 mmol) by the general procedure gave **8r** (49 mg, 13%) as a pale yellow solid. mp 194–196 °C; ¹H NMR (400 MHz, *d*₆-DMSO): δ 9.29 (s, 1H), 7.92 (q, *J* = 5.5 Hz, 1H), 7.87–7.83 (m, 1H), 7.81 (s, 1H), 7.76 (d, *J* = 8.2 Hz, 2H), 7.20 (d, *J* = 8.2 Hz, 2H), 6.39 (s, 1H) ¹³C NMR (100 MHz, *d*₆-DMSO): δ 167.0, 142.5, 141.8, 134.5, 134.4, 130.6, 127.8, 126.7, 126.6, 121.7, 110.0. HRMS (FAB): M+Na⁺, found 269.0241. C₁₃H₁₀O₂SNa⁺ requires 269.0243.

4.1.15. 3-[4-(2-Carboxyethenyl)phenyl]-2-hydroxy-2-propenoic acid (8s)

Hydrolysis of **6s** (369 mg, 1.34 mmol) by the general procedure gave **8s** (43 mg, 14%) as a mustard brown solid. mp > 220 °C; ¹H NMR (400 MHz, *d*₆-DMSO): δ 9.55 (s, 1H), 7.75 (d, *J* = 8.6 Hz, 2H), 7.61 (d, *J* = 8.6 Hz, 2H), 7.24 (d, *J* = 17.2 Hz, 1H), 6.45 (d, *J* = 17.2 Hz, 1H), 6.38 (s, 1H); ¹³C NMR (100 MHz, *d*₆-DMSO): δ 168.1, 166.5, 144.0, 143.2, 137.4, 130.0, 128.7, 128.5, 119.4, 108.9. HRMS (FAB): (M – H⁺) found 233.0453. (C₁₂H₁₀O₅ – H⁺) requires 233.0455.

4.1.16. 3-[3-(2-Carboxyethenyl)phenyl]-2-hydroxy-2-propenoic acid (8t)

From **6t** (389 mg, 1.29 mmol), gave **8t** (80 mg, 24%) as a yellow solid. mp 189 °C (dec.); ¹H NMR (400 MHz, *d*₆-DMSO): δ 9.41 (s, 1H), 7.94 (s, 1H), 7.82 (d, *J* = 7.7 Hz, 1H), 7.53 (d, *J* = 8.6 Hz, 1H), 7.50 (s, 1H), 7.36 (t, *J* = 7.7 Hz, 1H), 7.22 (d, *J* = 16.1 Hz, 1H), 6.46 (d, *J* = 16.2 Hz, 1H), 6.40 (s, 1H); ¹³C NMR (100 MHz, *d*₆-DMSO): δ 168.0, 166.6, 144.3, 143.0, 138.6, 136.2, 134.6, 131.1, 129.4, 127.1, 126.0, 119.7. HRMS (FAB): (M + Na⁺) found 257.0421. C₁₂H₁₀O₅Na⁺ requires 257.0420.

4.1.17. 3,3'-(1,4-Phenylene)bis[2-hydroxy-2-propenoic acid] (8u)

Hydrolysis of **6u** (443 mg, 1.77 mmol) by the general procedure gave **8u** (122 mg, 33%) as a dark yellow solid. mp 210 °C (dec.); ¹H NMR (400 MHz, *d*₆-DMSO): δ 9.29 (s, 2H), 7.69 (s, 2H), 7.14 (d, *J* = 8.0 Hz, 2H), 6.35 (s, 2H); ¹³C NMR (100 MHz, *d*₆-DMSO) δ 166.7, 142.4, 134.3, 129.6, 109.8. HRMS (FAB): M+Na⁺, found 273.0369. C₁₂H₁₀O₆Na⁺ requires 273.0370.

4.2. Enzyme inhibition assays

4.2.1. Screening compounds for inhibition using Fast Violet B

Compounds were initially screened for inhibition of *S. aureus* PC (SaPC) with an optimized assay that is based on the reaction of OAA, the product of the PC-catalyzed reaction, with Fast Violet B, a diazonium salt which produces a colored adduct with an absorbance maximum at 530 nm.¹¹ The published 96-well plate procedure was modified to a 384-well plate format such that all of the steps were identical

except that the volumes were decreased by half to a final assay volume of 60 μL . Assay conditions consisted of 50 mM Bis-Tris (pH 7.7), 3 mM MgCl_2 , 150 mM KCl, 1% DMSO and 0.5% Triton x-100. To determine whether the compounds interfered with formation of the FVB-OAA colored adduct itself, the procedure was modified slightly: 15 μL of OAA was added to a final concentration of 200 μM in place of 15 μL enzyme. This functioned to assess for possible interference of the compounds with the formation of the FVB-OAA adduct. None of the described compounds interfered with the FVB assay signal at 200 μM (Supplementary Table S1).

4.2.2. Measurement of OAA formation with malate dehydrogenase

Malate dehydrogenase coupled enzyme assays were performed at 22 $^\circ\text{C}$ in a 96-well plate format for a total reaction volume of 200 μL . Assay conditions consisted of 100 mM Tris (pH 7.8), 7 mM MgCl_2 , 150 mM KCl and 0.5% Triton x-100. First, 20 μL PC was added such that the final concentration in the assay was 10 $\mu\text{g}/\text{mL}$. Subsequently, 20 μL of compound was added to obtain the desired final concentration, 20 μL of MDH was added such that the final concentration in the assay was 20 U/mL, and lastly 140 μL of substrates were added to initiate the reaction (pyruvate, HCO_3^- , ATP and NADH to a final assay concentration of 12 mM, 25 mM, 2.5 mM and 0.25 mM, respectively). To assess the inhibition with respect to pyruvate, the procedure was modified such that 20 μL of pyruvate was added to the desired final concentrations prior to the addition of 120 μL of substrates to initiate the reaction (HCO_3^- , ATP and NADH to a final assay concentration of 25 mM, 2.5 mM and 0.25 mM, respectively). To assess the inhibition with respect to ATP, the procedure was modified such that 20 μM of ATP was added to the desired final concentrations prior to the addition of 120 μL of substrates to initiate the reaction (HCO_3^- , ATP and NADH to a final assay concentration of 25 mM, 12 mM and 0.25 mM, respectively). To account for possible compound inhibition of MDH (see Supplementary Table S1), the procedure was modified such that 20 μL OAA was added to a final concentration of 30 mM, in place of PC. Reagents were dispensed manually by a hand-held, multi-channel micropipette and absorbance measurements were recorded at 340 nm with a Multiskan Ascent spectrophotometer (Thermo).

4.2.3. Evaluation against human carbonic anhydrase (hCAII)

Assays for human carbonic anhydrase activity were performed in a 96-well plate format for a total reaction volume of 100 μL , in an assay modified from Day and Cohen.¹⁸ All assay reagents and solutions were prepared separately and maintained at 22 $^\circ\text{C}$ until warmed to 30 $^\circ\text{C}$. All substrates, effectors, and enzyme were freshly dissolved and diluted in assay buffer containing 50 mM Tris (pH 8.0). The final concentration of the human carbonic anhydrase II enzyme was 200 nM. Where noted, acetazolamide was included at a final concentration of 10 μM . The substrate, *p*-nitrophenyl acetate, was added at a final concentration of 504 μM . For all experiments, 20 μL of enzyme stock solution was added to each well in a 96-well, flat-bottom, polystyrene microplate (Santa Cruz Biotechnology) followed by the addition of 10 μL of the effectors (assay buffer for the uninhibited reaction, acetazolamide for inhibition). The 96-well plate was then incubated in a plate reader at 30 $^\circ\text{C}$ for 10 min; concurrently, the substrate solution was also warmed to 30 $^\circ\text{C}$ for 10 min. The enzymatic reaction was initiated by adding 70 μL of the substrate solution (*p*-nitrophenyl acetate). The absorbance values were then measured at 405 nm every 30 s over a period of 20 min for a total of 40 measurements.

4.2.4. Evaluation against matrix metalloproteinase-2 (MMP-2)

Assays for human matrix metalloproteinase-2 activity were performed in a 96-well plate format for a total reaction volume of 100 μL , in an assay modified from Day and Cohen.¹⁸ All assay reagents were prepared and maintained at 22 $^{\circ}\text{C}$ until warmed to 37 $^{\circ}\text{C}$. The omniMMP fluorogenic substrate and MMP-2 enzyme were prepared in assay buffer (50 mM HEPES, 10 mM CaCl_2 , 0.05% Brij-35, pH of 7.52), and small molecule effectors were prepared as a solution in 50% DMSO, 50% assay buffer. The final concentration of enzyme in the 100 μL enzymatic reaction was 0.0083 U/ μL . A known inhibitor, *N*-[(4'-bromo[1,1'-biphenyl]-4-yl)sulfonyl]-L-valine (PD166793), was included where noted at a final concentration of 100 μM . OmniMMP fluorogenic substrate was added to the 100 μL enzymatic reaction at a final concentration of 4 μM . For all experiments, 30 μL of enzyme stock solution was added to each well in a 96-well, flat-bottom, black polystyrene microplate (SantaCruz Biotechnology), followed by the addition of 10 μL of the effectors (50% assay buffer, 50% DMSO for the uninhibited reaction, PD166793 for inhibition). The 96-well plate was then incubated in a plate reader at 37 $^{\circ}\text{C}$ for 30 min; concurrently, the substrate solution was also warmed to 37 $^{\circ}\text{C}$ for 30 min. The enzymatic reaction was initiated by adding 60 μL of the omniMMP fluorogenic substrate solution. The change in fluorescence was then monitored for 30 min with excitation and emission wavelengths at 320 and 400 nm, respectively, every 46 s for a total of 40 measurements.

4.3. Computational docking

The ligand structures were built using ChemDraw (PerkinElmer) and saved as MDL Molefiles. The docking studies were performed using the docking program FITTED within the web-based FORECASTER platform,¹⁹ using the workflow "Docking-2D Molecules to a Rigid Protein (pdb)" which converts the 2D MDL Molefile to a 3D molecule and the protein pdb file (pdb code 3BG5) to a mol2 file. Protein Rotamer Elaboration and Protonation based on Accurate Residue Energy, or PREPARE, was utilized as part of the FITTED workflow. This software prepared all the atom files from the pdb files for suitable mol2 files. In addition to preparing the pdb files, PREPARE identified pyruvate in the pdb file by the residue name (PYR), chain location (A for open or C for closed conformation), and residue number (2001). The protein (as a mol2 file) was subsequently processed by PROtein Conformational Ensemble System Setup, or PROCESS, in the FITTED workflow to dock the 3D compounds in the binding site of the CT domain. The center of the binding site was defined by the center of pyruvate present in the active site. After the removal of pyruvate from the active site, a sphere with a radius of 15 \AA was applied as the default for establishing the binding site cavity. FITTED utilized a genetic algorithm/hybrid matching algorithm to dock the compounds within the established cavity site. Docking scores were reported from FITTED as the predicted binding energy (ΔG) and, following computational docking, the lowest energy pose was visualized in Pymol.

Acknowledgments

Financial support for this research was provided by the Marquette University Strategic Innovation Fund. We thank Prof. Nicolas Moitessier (McGill University) for providing access to the FITTED docking software in the FORECASTER platform.

Appendix A. Supplementary data

The following are the Supplementary data to this article: [Download : Download Acrobat PDF file \(660KB\)](#)

for download under the CC BY NC 3.0 licence

Data for: Evaluation of alpha-hydroxycinnamic acids as pyruvate carboxylase inhibitors

Supplementary Table S1. % Interference of FVB and MDH assay signals

Supplementary Figure S1. Inhibition of *S. aureus* pyruvate carboxylase (Michaelis-Menten)

Supplementary Figure S2. Lactate dehydrogenase (LDH) inhibition

Supplementary Figure S3. The ability of LDH to accept the compounds as...

Dataset

625KB

Supporting information.pdf

[View dataset on Mendeley Data](#)

[About research data](#)

References

- 1 S. Jitrapakdee, M. St. Maurice, I. Rayment, W.W. Cleland, J.C. Wallace, P.V. Atwood, *Biochem J*, 413 (2008), pp. 369-387
- 2 (a) T. Cheng, J. Sudderth, C. Yang, *et al.*, *Proc Natl Acad Sci USA*, 108 (2011), pp. 8674-8679 (b) N. Kumashiro, S.A. Beddow, D.F. Vatner, *et al.*, *Diabetes*, 62 (2013), pp. 2183-2194 (c) J. Shar, R. Stoll, K. Schauer, *et al.*, *J Bacteriol*, 192 (2010), pp. 1774-1784
- 3 (a) P.H. Choi, T.M.N. Vu, H.T. Pham, J.J. Woodward, M.S. Turner, L. Tong, *Proc Natl Acad Sci*, 114 (2017), pp. e7226-e7235 (b) A.T. Whitely, J.E. Garelis, B.N. Peterson, P.H. Choi, J.J. Tong, *Mol Microbiol*, 104 (2017), pp. 212-233 (c) G. Ferrandina, B. Melichar, A. Loercher, *et al.*, *Cancer Res*, 57 (1997), pp. 4309-4315 (d) T. Wilmanski, X. Zhou, W. Zheng, *et al.*, *Cancer Lett*, 411 (2017), pp. 171-181
- 4 (a) S. Farfari, V. Schulz, B. Corkey, M. Prentki, *Diabetes*, 49 (2000), pp. 718-726 (b) D. Lu, H. Mulder, P. Zhao, *et al.*, *Proc Natl Acad Sci*, 99 (2002), pp. 2708-2713
- 5 (a) L.E. Harrison, D.C. Wojciechowicz, M.F. Brennan, P.B. Paty, *Surgery*, 124 (1998), pp. 541-550 (b) J.H. Park, M.Y. Park, H.S. Park, *et al.*, *Cancer Res Treat*, 36 (2004), pp. 324-329 (c) K. Pahan, F.G. Sheikh, A.M. Namboodiri, I. Singh, *J Clin Invest*, 100 (1997), pp. 2671-2679
- 6 L. Tong, *Cell Mol Life Sci*, 70 (2013), pp. 863-891
- 7 A.D. Lietzan, M. St. Maurice, *Arch Biochem Biophys*, 544 (2014), pp. 75-86
- 8 G.J. Goodall, G.S. Baldwin, J.C. Wallace, D.B. Keech, *Biochem J*, 199 (1981), pp. 603-609
- 9 (a) S. Xiang, L. Tong, *Nat Struct Mol Biol*, 15 (2008), pp. 295-302 (b) P.V. Atwood, P.A. Tipton, W.W. Cleland, *Biochemistry*, 25 (1986), pp. 8197-8205

- 10 (a) A.D. Lietzan, M. St. Maurice, *Biochem Biophys Res Commun*, 441 (2013), pp. 377-382 (b) A.D. Lietzan, Y. Lin, M. St. Maurice, *Arch Biochem Biophys*, 562 (2014), pp. 70-79
- 11 B.N. Wyatt, L. Arnold, M. St. Maurice, *Anal Biochem*, 550 (2018), pp. 90-98
- 12 (a) L.A. Nickerson, V. Huynh, E.I. Balmond, S.P. Cramer, J.T. Shaw, *J Org Chem*, 81 (2016), pp. 11404-11408 (b) L.M. Weinstock, R.B. Currie, A.V. Lovell, *Synthetic Comm*, 11 (1981), pp. 943-946
- 13 (a) J.C. Thenmozhiyal, P.T. Wong, W.K. Chui, *J Med Chem*, 47 (2004), pp. 1527-1535 (b) K. Furukawa, H. Inada, M. Shibuya, Y. Yamamoto, *Org Lett*, 18 (2016), pp. 4230-4233 (c) D. Balducci, P.A. Conway, G. Sapuppo, H. Muller-Bunz, F. Paradisi, *Tetrahedron*, 68 (2012), pp. 7374-7379 (d) C. Avendano, E. de la Cuesta, L. Huck, I. Ortin, J.F. Gonzalez, *ARKIVOC*, iii (2011), pp. 200-211 (e) F. Bailly, C. Queffelec, G. Mbemba, *et al.*, *Eur J Med Chem*, 43 (2008), pp. 1222-1229 (f) P. Busca, F. Paradisi, E. Moynihan, A.R. Maguire, P.C. Engle, *Org Biomol Chem*, 2 (2004), pp. 2684-2691
- 14 T. Takai, H. Senda, H.H. Lee, *Spectroscopy Lett*, 31 (1998), pp. 379-395
- 15 A.D. Lietzan, M. St. Maurice, *J Biol Chem*, 288 (2013), pp. 19915-19925
- 16 (a) B.A. Patel, C.B. Ziegler, N.A. Cortese, *et al.*, *J Org Chem*, 42 (1977), pp. 3903-3907 (b) A. Tanaka, T. Terasawa, H. Hagihara, *et al.*, *J Med Chem*, 41 (1998), pp. 2390-2410
- 17 L. Zhu, Q. Meng, W. Fan, X. Xie, Z. Zhang, *J Org Chem*, 75 (2010), pp. 6027-6030
- 18 J.A. Day, S.M. Cohen, *J Med Chem*, 56 (2013), pp. 7997-8007
- 19 E. Therrien, P. Englebienne, A.G. Arrowsmith, *et al.*, *J Chem Inf Model*, 52 (2012), pp. 210-224